Compact Structure with Three Attenuation Poles for Harmonics Suppression

Rui Li · Dong Il Kim* · Chang Mook Choi* · Dae Hee Lee* · Yong Man Song**

** Department of Radio Sciences and Engineering, Korea Maritime University, Busan 606-791, Korea*

ABSTRACT : *A novel compact structure with three controllable finite attenuation poles at stopband is presented. The new compact structure is composed of a pair of symmetrical parallel coupled-line and a capacitive load. With this configuration, three finite attenuation poles are available, which can improve the stopband characteristics of low-pass filters or the upper stopband performances of band-pass filters. The research method is based on transmission-line model for tuning the finite attenuation poles. In order to examine the feasibility of the proposed structure, a new type of low-pass filter with broad stopband and sharp cutoff frequency response is designed, fabricated, and measured. The experimental results of the fabricated circuit agree well with the simulation and analytical ones.*

KEY WORDS : Band-pass filter (BPF), capacitive load, finite attenuation pole, low-pass filter (LPF), parallel coupled-line

1. Introduction

The low-pass filters are often employed in many communication systems to suppress harmonic and spurious signals, with the demand for compact size, low insertion loss, and high attenuation. The conventional low-pass filters, such as open-circuited stub low-pass filters and stepped impedance low-pass filters can not meet the requirements for modern communication systems because of their large size and narrow stopband. For sharper cutoff and high attenuation at stopband, the order of the stepped-impedance low-pass filter must be very high [1][2], thereby the circuit size and insertion loss will be increased. In literature, many design approaches have been proposed to improve the low-pass filter's performance. The low-pass filters using PBG and DGS structures [3][4] that can improve the skirt characteristic and provide wide and deep

* zcrlr@hotmail.com 051)410-4932,
* dikim@mail.hhu.ac.kr 051)410-4314,
* nav-sun@hanmail.net 051)410-4932,
* sjsj-0517@hanmail.net, 051)410-4932

stopband as compared with the conventional low-pass filters. A low-pass filter using multiple cascaded hairpin resonators that can provide sharp cutoff frequency responses with low passband insertion loss has been demonstrated in [5][6]. However, this type of design approach is a little complicated and just used to synthesize some parts of available prototype low-pass filters.In this paper, a novel and more compact structure with three controllable finite attenuation poles at stopband is proposed and a new type of low-pass filter based on this structure, which consists of a pair of symmetrical parallel coupled-line and a capacitive load, is developed. The proposed approach demonstrates many attractive features: simple and compact structure, low passband insertion loss, broad stopband, and sharp skirt characteristic.

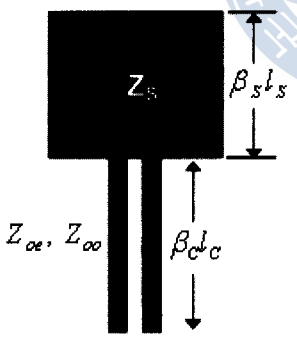

Fig. 1 Layout of the proposed compact low-pass filter

2. Finite Attenuation Poles Analysis

Fig. 1 shows the basic layout of the proposed compact structure. It consists of a capacitive load C_S and a pair of symmetrical parallel coupled-line with a length of l_c. Z_{oe} and Z_{oo} represent the even- and odd-mode characteristic impedances of the parallel coupled-line, respectively. For analyzing this circuit easily, we assume that the structure is lossless and the width of the feeding lines is negligible. Under these assumptions, the proposed structure can be divided into two sections: one is capacitive load section and the other is symmetrical parallel coupled-line section with its far end shorted. As shown in Fig. 2(a), the total Z-matrix of a serially connected network can be given by [2]

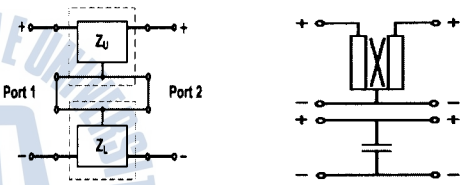

Fig. 2 (a) Serially connected two-port network. (b) Decomposition diagram of the proposed structure

$$[Z_T]=[Z_U]+[Z_L] \tag{1}$$

where $[Z_U]$ and $[Z_L]$ are the impedance matrices of the upper and lower network, respectively. As depicted in Fig. 2(b), the coupled-line and the capacitive load sections can be seen as the upper and lower networks, respectively. For the upper network, the elements of the impedance matrix $[Z_U]$ can be calculated by using even-odd mode analysis method as following:

$$Z_{11}^{U} = j(Z_{oe}\tan\theta_e + Z_{oo}\tan\theta_o)/2 \tag{2a}$$

$$Z_{21}^{U} = j(Z_{oe}\tan\theta_e - Z_{oo}\tan\theta_o)/2 \quad (2b)$$

For the lower network, the elements of the impedance matrix are the same and can be derived as:

$$Z_{mn} = -j/(\omega C_S), \quad m,n=1,2. \quad (3)$$

From the relationship between the impedance and scattering matrices, the transmission parameter of the network can be obtained by [7]

$$S_{21} = \frac{2Z_{12}^{T}Z_0}{(Z_{11}^{T}+Z_0)(Z_{22}^{T}+Z_0)-Z_{12}^{T}Z_{21}^{T}} \quad (4)$$

where Z_0 is the input and output microstrip line characteristic impedance. The finite attenuation poles are located at the angular frequencies ω where $S_{21}(\omega) = 0$ or $Z_{21}(\omega) = 0$. Therefore, the frequencies of the finite attenuation poles should satisfy the following equation derived from (2b) and (3):

$$(Z_{oe}\tan\theta_e - Z_{oo}\tan\theta_o)/2 = 1/\omega C_S \quad (5)$$

Inspecting (5), the frequencies of the finite attenuation poles can be determined by the capacitive load C_S and the electrical parameters of the parallel coupled-line. Fig. (3a) shows the pictorial descriptions of varying the capacitance C_S. There are three intersections between the upper reactance function X_U and the lower one X_L through the stopband. It means that three finite attenuation poles will be located through the stopband at the same frequencies as the intersections between the upper and lower reactance functions. As illustrated in Fig. (3b), the predicted results are confirmed by the simulated frequency responses. The locations of the transmission zeros are almost same as those of the intersections shown in Fig. 3(a). The simulated results with three different capacitance values demonstrate that the first and third finite attenuation poles shift to the upper frequency as the capacitance value decreases and the second finite attenuation pole has almost no-shift. Moreover, the slope factor of the cut-off transition is about the same. Therefore, the cut-off frequency can be adjusted easily by selecting an appropriate capacitive load, but without changing the sharpness of the cut-off.

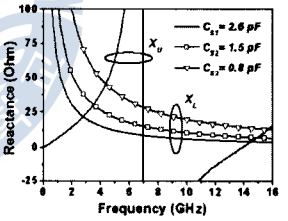

(a)

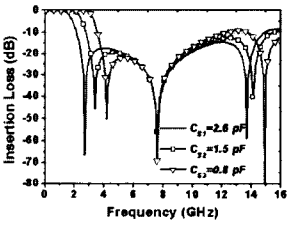

(b)

Fig. 3 Compact structure with different capacitive loads. (a) Pictorial reactance descriptions. (b) Simulated frequency responses with the following electrical parameters: l_C = 7.0 mm, s =0.5 mm, and w = 0.23 mm

The first and second finite attenuation poles, however, will be so close as to produce just one transmission zero when the capacitance value is selected to be small enough. To continuously inspect the effects on the frequency responses of the proposed structure caused by the parallel coupled-line, a comparison has been made among three different structures with different length of the parallel coupled-line based on same capacitive load. As shown in Fig. 4(a), all three intersections shift to the upper frequency as the length of the coupled-line decreases gradually, especially the second and third ones. The frequency responses demonstrated in Fig. 4(b) also present the same characteristics. Furthermore, from the partial enlarged view as depicted in Fig. 4(c), as the length of the coupled-line increases, the cut-off sharpness becomes more abrupt.

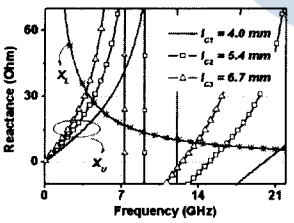

(a)

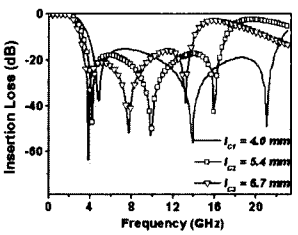

(b)

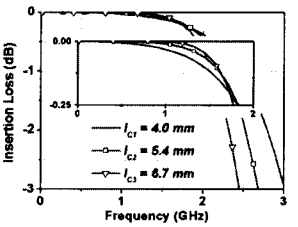

(c)

Fig. 4 Compact structure with different length of the parallel coupled-line. (a) Pictorial reactance descriptions. (b) Simulated frequency responses with the following electrical parameters: C_S = 1.3 pF, s = 0.5 mm, and w = 0.23 mm. (c) Partial enlarged view

3. Application of the Proposed Structure

By the above graphic analysis, the proposed compact structure can provide a wide rejection band with three finite attenuation poles, and these finite attenuation poles can be adjusted easily just by changing the capacitive load value and the length of the coupled-line. The attractive feature can be used to improve the stopband characteristics of low-pass and band-pass filters for harmonics and spurious suppression. To verify the proposed approach, a low-pass filter with its cutoff frequency at 2.0 GHz is developed. The low-pass filter is designed and fabricated on a 0.76 mm thick Taconic PCB with a relative dielectric constant of εr = 3.5. The capacitive load can be a monolithic multi-layered ceramic capacitor or a metal-insulator-metal capacitor. In this case, we select an open-circuited stub to be the capacitive load for simple fabrication

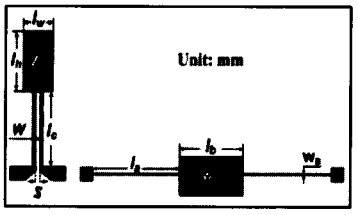

(a)

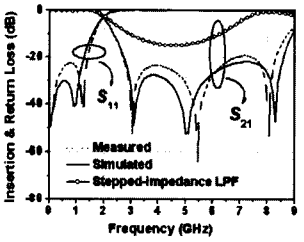

(b)

Fig. 5 (a) Layout comparison between the proposed and the conventional stepped-impedance low-pass filters. (b) Simulated and measured results

Table 1 Comparison of the physical dimensions

Proposed LPF		Stepped-impedance LPF	
Coupled-line (mm)	Capacitor (pF)	High-Z line (mm)	Low-Z line (mm)
Length : 13	Cs : 1.5	Length : 11.51	Length : 8.45
Width : 0.4			
space : 0.4		Width: 0.22	Width : 4.54
Substrate thickness : 0.76 mm, relative dielectric : 3.5			

and low insertion loss [7]. By applying the rules examined in Section II, as well as optimized by Ansoft HFSS Simulator for considering the discontinuity effect at a step between the open-circuited stub and the parallel coupled-line, the physical dimensions of the circuit, as depicted in Fig. 5(a), are finally determined as: *l*w = 4.0 mm, *l*h = 7.0 mm, *l*c = 9.0 mm, w = 0.25 mm, and s = 0.36 mm.

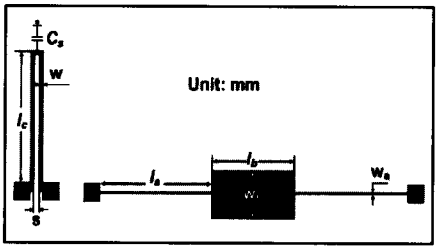

(a) (b)

Fig. 6 Layouts of (a) the proposed low-pass filter and (b) conventional stepped-impedance low-pass filter

The fabricated low-pass filter is measured with Anritsu 37369D vector network analyzer. As shown in Fig. 5(b), the measured results agree well with the simulated ones. This low-pass filter has a 3-dB cutoff frequency at 1.99 GHz. The insertion loss is lower than 0.5 dB from DC to 1.6 GHz. The rejection band is extended from 2.7 to 8.35 GHz over 20 dB, and three finite attenuation poles are located at 3.05, 5.45, and 8.05 GHz with 52.5, 64.1, and 53 dB, respectively. In this paper, we also develop a new kind of semi-lumped compact low-pass filter to suppress 1st, 2nd, and 3rd harmonics. In this case, a chip capacitor is used to replace the open-stub as the load capacitor in order to reduce the effective circuit area. By using the same optimizing method proposed in the fore mentioned design. A semi-lumped low-pass filter with its cutoff frequency at 1.3 GHz is developed. The electrical parameters of the parallel coupled-line and shunted capacitor are selected to suppress the 2nd, 3rd, and 4th harmonics, simultaneously. A compact low-pass filter is designed and fabricated on a 0.76 mm thickness Taconic PCB with a relative dielectric constant of εr = 3.5.

Adjusting the locations of the reactance intersections by adjusting the circuit parameters, as well as optimized by Agilent ADS software, the circuit electrical parameters are determined as shown in Table I, and a comparison of the circuit layouts between the proposed compact low-pass filter and the conventional stepped impedance one has been made as illustrated in Fig. 6.

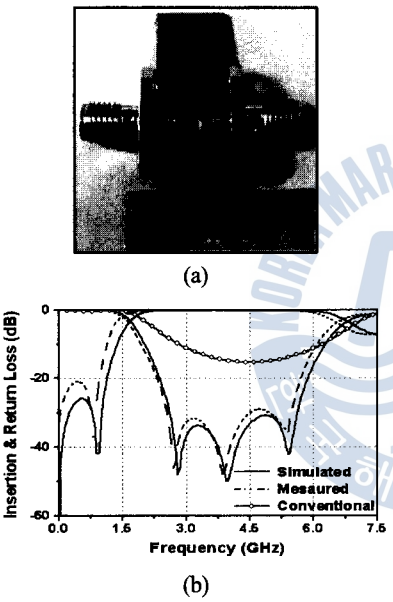

Fig. 7 Proposed compact low-pass filter. (a) Photograph of the fabricated circuit.(b) Measured frequency responses compared with those of the simulated and conventional stepped-impedance low-pass filter

A photograph of the fabricated semi-lumped low-pass filter is shown in Fig. 7(a). The fabricated low-pass filter was measured with Anritsu 37369D vector network analyzer. As shown in Fig. 7(b), the measured results agree well with the simulated ones. This low-pass filter has a 3-dB cutoff frequency at 1.3 GHz. The three finite attenuation poles at stopband are located at 2.7 GHz, 3.85 GHz, and 5.35 GHz with insertion losses of 46 dB, 47.9 dB, and 35.5 dB, respectively. The locations are almost same as the 2nd, 3rd, and 4th harmonics of the cutoff frequency. Thereby the harmonics can be eliminated effectively. Moreover, any of the unwanted frequencies can be eliminated using this kind of circuit by adjusting the electrical circuit parameters effectively.

4. Conclusion

A new compact structure with three finite attenuation poles at stopband has been proposed in this paper. Through theoretical analysis and simulation performances, the cut-off sharpness and rejection band can be controlled by adjusting the circuit electrical parameters easily. To verify the feasibility of the proposed method, a one-stage low-pass filter has been designed, fabricated, and measured. based on our observations of simulation performances and measurement, this new type of low-pass filter demonstrated many desirable features as compared with the conventional one, such as compact structure, sharp skirt characteristic, and wide stopband with three controllable finite attenuation poles. In addition, the proposed approach can be further extended and used in cascaded filters design to achieve much sharper skirt characteristic and broad

rejection-band with much higher attenuation level. The compact structure proposed in this paper is very useful for applications in modern communications systems.

Acknowledgement

This work was supported by the Korea Research Foundation Grant funded by the Korean Government (KRF-2005-005-J00502).

References

[1] G. L. Mattaei, L. Young, and E. M. T. Jones, Microwave Filters, Impedance Matching Networks and Coupling Structures. New York: McGraw-Hill, pp. 223-410, 1980.

[2] J. Sheng Hong and M. J. Lancaster, Microstrip Filters for RF/Microwave Applications. New York: Wiley, pp. 14-16, 2001.

[3] I. Rumsey, M. Piket-May, and P. K. Kelly, "Photonic Bandgap Structure used as Filters in Microstrip Circuits," IEEE Microw. Guided Wave Lett., vol. 8, no. 10, pp. 336-338, Oct. 1998.

[4] D. Ahn, J. S. Park, C. S. Kim, J. Kim, Y. Qian, and T. Itoh, "A Design of the Low-Pass Filter Using the Novel Microstrip Defected Ground Structure," IEEE Trans. Microw. Theory Tech., vol. 49, no.1, pp. 86-93, Jan. 2001.

[5] L.-H Hsieh and K. Chang, "Compact Low-pass Filter Using Stepped Impedance Hairpin Resonator," Electron. Lett. vol. 37, no.14, pp. 899-900, July. 2001.

[6] L.-H Hsieh and K. Chang, "Compact Elliptic-Function Low-pass Filters Using Microstrip Stepped-Impedance Hairpin Resonators," IEEE Microw. Theory Tech., vol. 51, no.1, pp. 193-199, Jan. 2003.

[7] David M. Pozar, Microwave Engineering, 3rd ed. New York: Wiley, 2005.

Received : 26 December 2006
Accepted : 19 January 2007